Available online at www.sciencedirect.com
ScienceDirect
Journal of Sound and Vibration 300 (2007) 453–465
JOURNAL OF SOUND AND VIBRATION
www.elsevier.com/locate/jsvi

Analysis of the dynamic stability of collar-stiffened pipes conveying fluid

Osama J. Aldraihem*

Mechanical Engineering Department, King Saud University, PO 800, Riyadh 11421, Kingdom of Saudi Arabia

Received 12 July 2004; received in revised form 20 December 2005; accepted 1 March 2006
Available online 28 November 2006

Abstract

The dynamic stability of a collar-stiffened pipe conveying fluid was examined by using the Euler–Bernoulli beam theory. The pipe considered consists of identical substructures, or cells, connected in an identical fashion. Each substructure, or cell, comprises a uniform pipe segment and a collar. A finite element model was developed to predict the dynamic stability of the stiffened pipe under the action of the flowing fluid. Stability maps were obtained for clamped-free collar-stiffened pipes of various design parameters. The design parameters included the arrangement and the geometry of the identical cells. The stability maps demonstrated that the collar-stiffened pipe exhibits unique stability characteristics when compared to a uniform pipe. It was found that the stable region in the stability map enlarges for the collar-stiffened pipe when compared to a uniform pipe. To give clearer insight into the pipe dynamic behavior, the dynamic response and eigenvalue branches were presented for a number of collar-stiffened pipes.

1. Introduction

The dynamic stability of pipes conveying fluid has been a challenging problem over the last century. The instability of a pipe is initiated when the fluid is transported at a critical speed through the pipe system. Systems such as piping networks, feed tubes of rocket motors, tubes in heat exchangers and nuclear reactor components are some examples of pipes conveying fluid. The dynamic behavior of this class of structures is quantified by considering their dynamic response and dynamic stability. In the dynamic response analysis, the system behavior is determined in the time and/or frequency domain. The analysis of dynamic stability involves, however, the computation of the boundaries between the stable and unstable regions. In the appropriate planes of system parameters, a stability map is usually constructed to show the boundaries between the stable and unstable regions.

Considerable research effort has been put forth to study the dynamic response and stability of uniform pipes conveying fluid. For example, Housner [1] was the first to investigate the dynamic stability of uniform pipes supported at both ends and conveying fluids. Benjamin [2] was the first to correctly derive Hamilton's principle of continuous, flexible, pipes. The work of Gregory and Païdoussis [3,4] focused on obtaining

*Corresponding author. Tel.: +966 1 467 6671; fax: +966 1 467 6652.
E-mail address: odraihem@ksu.edu.sa.

0022-460X/$ - see front matter © 2006 Elsevier Ltd. All rights reserved.
doi:10.1016/j.jsv.2006.09.007

Nomenclature

A	cross-sectional area
$\mathbf{A}$	system matrix in Eq. (18)
$\dot{c}$	axial velocity of the pipe
$\mathbf{C}$	global damping matrix of the pipe
$\mathbf{C}_f$	skew damping matrix due to flowing fluid
$\mathbf{C}_{\text{ou}}$	damping matrix due to fluid out-release
D_i	inner diameter of the pipe
D_{o}	outer diameter of the pipe
E	Young's modulus
f	step factor in Fig. 1(b)
$\mathbf{f}_g$	load vector in Eq. (14)
$\mathbf{F}$	state space load vector in Eq. (23)
g	gravitational acceleration
h	finite element length
I	moment of inertia
$\mathbf{K}$	global stiffness matrix of the pipe
$\mathbf{K}_f$	stiffness matrix due to flowing fluid
$\mathbf{K}_{\text{ou}}$	stiffness matrix due to fluid out-release
L	pipe length
Lu	cell length
Ls	collar length
m_f	fluid mass per unit length
$\mathbf{M}$	global mass matrix of the pipe
n	number of finite elements
N_i	shape functions
t	time
T	total kinetic energy of the pipe system
T_p	kinetic energy of the pipe
T_f	kinetic energy of the fluid
U	fluid speed relative to the pipe
u	dimensionless speed ratio $= UL\sqrt{m_f/EI}$
V	total strain energy of the pipe system
v_i	nodal DOF
v_x	x-component of the fluid absolute velocity
v_z	z-component of the fluid absolute velocity
v	vector of nodal displacements
W_{nc}	work of non-conservative forces
w	transverse displacement of the pipe
x	global x coordinate
$\mathbf{Z}$	state space vector in Eq. (19)

Greek letters

β	dimensionless mass ratio $= m_f/(m_f+\rho A)$
δ	first variation
η	damping coefficient of the pipe material
λ	eigenvalue of the system matrix $\mathbf{A}$
ρ	mass density of the pipe
ζ	time variable in Eq. (24)

Superscripts

T	transpose
$(\bullet)'$	spatial derivative $= \partial(\bullet)/\partial x$
$(\dot{\bullet})$	time derivative$= \partial(\bullet)/\partial t$

the stability conditions of uniform cantilever pipes. Païdoussis [5] has presented a comprehensive survey of the dynamics and stability of slender structures subjected to moving fluid. Païdoussis and Li [6] reviewed the dynamics of pipes conveying fluid and presented a selective review of the research undertaken on it. Pandiyan and Sinha [7] presented procedure for the analysis of nonlinear dynamical systems with periodically varying parameters under critical conditions. Semler et al. [8] used energy and Newtonian methods to derive the nonlinear equations of motion of pipes conveying fluid. In a more recent work, Semler and Païdoussis [9] presented an overview of the applicability of some numerical approaches in parametric resonances of cantilevered pipes. Szabo [10] investigated the dynamic behavior of pipe containing pulsatile flow.

The literature regarding the stability analyses of stepped pipes conveying fluid is limited. A work by Maalawi and Ziada [11] is focused on the static instability of stepped pipes conveying fluid. In their study [11], each uniform portion of the pipe is considered as a module and the instability is investigated when the module's wall thickness and length is changed. In a related problem, Aldraihem and Baz [12,13] studied the dynamic stability of stepped beams under the action of moving loads. It has been shown that better stability characteristics can be obtained by using stepped beam when compared to a uniform beam.

The present paper had the objective of presenting a general stability analysis for collar-stiffened pipe consisting of substructures or cells. Each substructure or cell comprises a uniform pipe segment and a collar. A finite element model was formulated to account for the collars and the interaction between the flowing fluid and pipe vibration. The stability of the collar-stiffened pipe is evaluated by analyzing the eigenvalues of the collar-stiffened pipe system. The dynamic stability of collar-stiffened cantilever pipes conveying fluid was

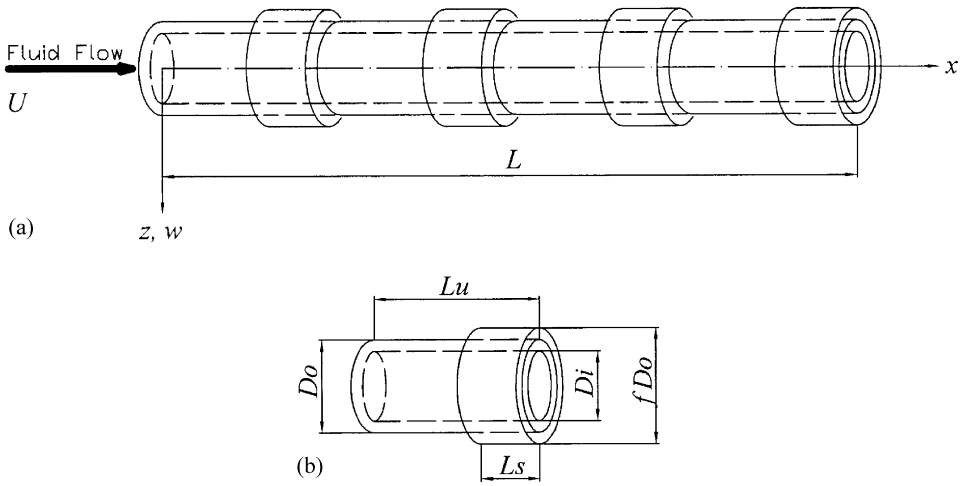

Fig. 1. Collar-stiffened pipe (a) and one cell geometry (b).

investigated. The effects of the number of cells, cell length ratio and step factor on the stability characteristics were demonstrated. The dynamic response and the eigenvalue branches (i.e. the modes of vibration that are responsible for causing instability in the pipe) are presented for a number of pipe systems.

2. Analysis

The system considered consisted of a collar-stiffened pipe of length L, as shown in Fig. 1(a). The pipe conveyed a fluid moving at a constant axial velocity relative to the pipe U. The pipe consisted of identical cells, or substructures, connected in identical fashion (Fig. 1(a)). Each cell comprised a uniform pipe segment and a collar which is perfectly attached to the outer-surface of the cell. The length of the cell is Lu, and the length of the collar is Ls (Fig. 1(b)). The pipe x-axis was assumed to pass through the centroid of the cross-section and to vibrate in the x–z plane.

The main assumptions for the collar-stiffened pipe and the moving fluid are as follows: (1) the pipe is symmetric and obeys the Euler–Bernoulli theory; (2) the fluid is incompressible and of mass m_f per unit length; and (3) the pipe's cells are made of isotropic materials.

2.1. Variational formulation

A variational approach, which accounts for the exchange of energy between a flowing fluid and a pipe, can be used. The approach was first devised by Benjamin [2] and then elaborated by McIver [14]. The approach is essentially Hamilton's principle with some modification to encompass the fluid energy exchange.

Adopting Benjamin's technique, the Hamilton's principle of a pipe conveying fluid can be written as [2]

$$\int_{t_1}^{t_2}\left\{\delta(T-V)+\delta W_{\mathrm{nc}}+m_f U^2\int_0^L w'\delta w'\,\mathrm{d}x-m_f U\left(\dot{w}_L+Uw'_L\right)\delta w_L\right\}\mathrm{d}t=0, \tag{1}$$

where δ is the first variation, T is pipe total kinetic energy, V is pipe strain energy, δW_{nc} is virtual work done by the non-conservative forces (which includes structural damping and forces not accounted for in V), w is the transverse displacement of the pipe. The primes denote spatial derivatives with respect to x and the dots denote time derivatives. The notation $w_L = w(L, t)$ is used.

2.1.1. Kinetic energy

The total kinetic energy of the pipe is the sum of the kinetic energy of the collar-stiffened pipe, T_p, plus the kinetic energy of the flowing fluid, T_f. The kinetic energy attributed to the collar-stiffened

pipe is given by

$$T_p = \frac{1}{2}\int_0^L \rho A \dot{w}^2 \, dx, \tag{2}$$

where ρ is the pipe mass density and A is the pipe cross-sectional area. It should be noted that the cross-sectional area for the uniform pipe portion is different from the collar portion.

The kinetic energy of the moving fluid is

$$T_f = \frac{1}{2} m_f \left[v_z^2 + v_x^2\right]. \tag{3}$$

Although the fluid velocity relative to the pipe is a constant U, the components of the absolute fluid velocity vary with time and are given by

$$\begin{aligned} \mathrm{v}_z &= \dot{w} + U w', \\ \mathrm{v}_x &= U\left[1 - \frac{1}{2}(w')^2\right] - \dot{c}, \end{aligned} \tag{4}$$

where $\dot{c}$ denotes the pipe velocity in the x direction.

From Eqs. (3) and (4) and neglecting the higher order terms (i.e., approximate to second order), the kinetic energy of the fluid reduces to

$$T_f = \frac{1}{2} m_f \int_0^L \left(\dot{w}^2 + 2U\dot{w}w' + U^2 - 2U\dot{c}\right) dx. \tag{5}$$

Hence, the total kinetic energy is obtained as

$$T = \frac{1}{2}\int_0^L \left[\rho A \dot{w}^2 + m_f\left(\dot{w}^2 + 2U\dot{w}w' + U^2 - 2U\dot{c}\right)\right] dx. \tag{6}$$

It should be noted that the last two terms in Eq. (6) will vanish with the first variation.

2.1.2. Strain energy

The strain energy of a collar-stiffened pipe can be expressed as

$$V = \frac{1}{2}\int_0^L \left[EI(w'')^2 - 2(\rho A + m_f)g\right] dx, \tag{7}$$

where E denotes the Young's modulus, I denotes the pipe moment of inertia and g denotes the gravitational acceleration. In Eq. (7), the moment of inertia is stepwise constant, i.e., it has value for the uniform pipe portion different from the collar portion.

2.1.3. Work by non-conservative forces

The work done by the non-conservative forces is only due to the internal damping of the pipe. In this study, the damping is assumed to follow the Kelvin–Voigt model that yields the following expression:

$$\delta W_{\mathrm{nc}} = -\int_0^L \eta I \dot{w}'' \delta w'' \, dx, \tag{8}$$

where η is the damping coefficient.

2.2. Distributed-parameter model

Using Eq. (1) with Eqs. (6)–(8) and performing some algebraic manipulations yields the following equation of motion:

$$\rho A \ddot{w} + EIw'''' = p_f(x,t) + p_d(x,t), \tag{9}$$

where the excitation load and the damping force are, respectively, given as

$$p_f(x,t) = -m_f\left(\ddot{w} - g + 2U\dot{w}' + U^2 w''\right) + \rho A g,$$
$$p_d(x,t) = -\eta I \dot{w}'''', \tag{10}$$

with boundary conditions pairs

	Essential BC	Natural BC
At $x = 0$	w	$\eta I\dot{w}''' + EIw''' = -m_f U(\dot{w} + Uw')$,
	w'	$\eta I\dot{w}'' + EIw'' = 0$,
At $x = L$	w	$\eta I\dot{w}''' + EIw''' = 0$,
	w'	$\eta I\dot{w}'' + EIw'' = 0$.

(11)

It should be emphasized that the shear natural boundary condition at $x = 0$ is different than that at $x = L$. This distinction is generated by the flow out-release effect. The parameters ρA, EI and ηI vary in stepwise manner along the pipe x-axis.

The terms on left-hand side of Eq. (9) are, respectively, the inertia force and the flexural force of the pipe. Starting from the equality sign, the various terms on the right-hand side of the excitation load $p_f(x,t)$ (Eq. (10)), may be identified, sequentially, as the fluid inertia, gravitational, Coriolis, and centrifugal forces, and the pipe gravitational force. The term $p_d(x,t)$ is a non-conservative damping force.

2.3. Finite element model

Investigating the dynamic behavior of the pipe system, Eqs. (9)–(11) analytically is found to be a difficult task. Approximate techniques such as finite element method will be used to examine the system stability and response. A one-dimensional (1D) beam element will be formulated to discretize the system equations. The shape functions used to approximate the transverse displacement are chosen to be Hermite-cubic polynomials. The displacements of the beam elements are approximated by

$$w(x,t) = \sum_{i=1}^{4} N_i(x) v_i(t), \tag{12}$$

where (v_1, v_2) and (v_3, v_4) are transverse displacement and rotation at the left end and the right end of the finite element, respectively, and N_i represent the shape functions given by

$$\mathbf{N}^{\mathrm{T}} = \begin{bmatrix} 1 - 3\left(\frac{x-x_i}{h}\right)^2 + 2\left(\frac{x-x_i}{h}\right)^3 \\ (x-x_i) - 2h\left(\frac{x-x_i}{h}\right)^2 + h\left(\frac{x-x_i}{h}\right)^3 \\ 3\left(\frac{x-x_i}{h}\right)^2 - 2\left(\frac{x-x_i}{h}\right)^3 \\ -h\left(\frac{x-x_i}{h}\right)^2 + h\left(\frac{x-x_i}{h}\right)^3 \end{bmatrix}, \tag{13}$$

where x denotes the pipe global x coordinate, x_i denotes the distance from the left end of the pipe to the left node of the ith finite element, and h denotes the length of the finite element.

For n finite elements the discrete differential equations of the collar-stiffened pipe are obtained by using Eq. (12) to evaluate the energy terms in the Hamilton's principle (Eq. (1)). Integrating the result over the spatial domains leads to

$$\mathbf{M}\ddot{v} + \left(\mathbf{C} + \mathbf{C}_f + \mathbf{C}_{\mathrm{ou}}\right)\dot{v} + \left(\mathbf{K} + \mathbf{K}_f + \mathbf{K}_{\mathrm{ou}}\right)v = \mathbf{f}_g, \tag{14}$$

where

$$\mathbf{M} = \int_0^L (\rho A + m_f)\mathbf{N}^{\mathrm{T}}\mathbf{N}\,\mathrm{d}x, \quad \mathbf{C} = \int_0^L \eta I \mathbf{N}''^{\mathrm{T}}\mathbf{N}''\,\mathrm{d}x,$$

$$\mathbf{K} = \int_0^L EI\mathbf{N}''^{\mathrm{T}}\mathbf{N}''\,\mathrm{d}x, \quad \mathbf{C}_f = \int_0^L m_f U\left(\mathbf{N}^{\mathrm{T}}\mathbf{N}' - \mathbf{N}'^{\mathrm{T}}\mathbf{N}\right)\mathrm{d}x,$$
$$\mathbf{C}_{\mathrm{ou}} = \mathbf{0}, \text{ except } \mathbf{C}_{\mathrm{ou}}(2n-1, 2n-1) = m_f U,$$
$$\mathbf{K}_f = -\int_0^L m_f U^2 \mathbf{N}'^{\mathrm{T}}\mathbf{N}'\,\mathrm{d}x,$$
$$\mathbf{K}_{\mathrm{ou}} = 0, \text{ except } \mathbf{K}_{\mathrm{ou}}(2n-1, 2n) = m_f U^2,$$
$$\mathbf{f}_g = \int_0^L (\rho A + m_f) g\mathbf{N}^{\mathrm{T}}\,\mathrm{d}x, \tag{15}$$

where $\mathbf{M}$, $\mathbf{C}$ and $\mathbf{K}$ matrices are the global mass, damping and stiffness matrices of the pipe, respectively; $\mathbf{f}_g$ is the gravitational load vector. It should be mentioned that the $\mathbf{C}_f$ matrix is a skew-symmetric matrix; i.e., $\mathbf{C}_f = -\mathbf{C}_f^{\mathrm{T}}$.

To simplify the presentation, Eq. (14) is expressed as

$$\mathbf{M}_{\mathrm{eq}}\ddot{v} + \mathbf{C}_{\mathrm{eq}}\dot{v} + \mathbf{K}_{\mathrm{eq}}v = \mathbf{f}_{\mathrm{eq}} \tag{16}$$

with

$$\mathbf{M}_{\mathrm{eq}} = \mathbf{M}, \quad \mathbf{C}_{\mathrm{eq}} = \left(\mathbf{C} + \mathbf{C}_f + \mathbf{C}_{\mathrm{ou}}\right),$$
$$\mathbf{K}_{\mathrm{eq}} = \left(\mathbf{K} + \mathbf{K}_f + \mathbf{K}_{\mathrm{ou}}\right) \quad \text{and} \quad \mathbf{f}_{\mathrm{eq}} = \mathbf{f}_g. \tag{17}$$

2.4. Stability analyses and dynamic response

The pipe under consideration may lose stability by either divergence (a static form of instability) or flutter (a dynamic form of instability) [5]. Divergence may occur if both ends of the pipe are restrained. If one end of the pipe is restraint free, flutter may occur in the pipe. To study the pipe stability, the homogeneous part of the second-order system (Eq. (16)), is cast in a first-order form:

$$\dot{\mathbf{Z}} = \mathbf{A}\mathbf{Z}, \tag{18}$$

where

$$\mathbf{Z} = \begin{pmatrix} v \\ \dot{v} \end{pmatrix} \text{ and } \mathbf{A} = \begin{bmatrix} 0 & \mathbf{I} \\ -\mathbf{M}_{\mathrm{eq}}^{-1}\mathbf{K}_{\mathrm{eq}} & -\mathbf{M}_{\mathrm{eq}}^{-1}\mathbf{C}_{\mathrm{eq}} \end{bmatrix}. \tag{19}$$

The behavior of the above system (Eq. (18)), in the neighborhood of the equilibrium depends upon the eigenvalues of the matrix $\mathbf{A}$. It is assumed that the solution of Eq. (18) has the form

$$\mathbf{Z} = \mathbf{e}^{\lambda t}\mathbf{B}, \tag{20}$$

where λ is a complex number to be determined and $\mathbf{B}$ is a constant vector. When the solution Eq. (20), is inserted into Eq. (18), the nontrivial solution of $\mathbf{B}$ is assured by making

$$|\mathbf{A} - \lambda\mathbf{I}| = 0. \tag{21}$$

Since the size of matrix $\mathbf{A}$ is $(4n \times 4n)$, Eq. (21) has $4n$ solutions. The stability of the collar-stiffened pipe is determined by the sign of the real part of the eigenvalue $\lambda\cdot$ If the real parts of the eigenvalues are negative, the pipe is asymptotically stable; if at least one of the eigenvalues has a positive real part, the pipe is unstable; if at least one of the eigenvalues has no real part, the pipe is marginally stable. Several methods are available to find the system eigenvalues. In this study, a MATLAB® operator is exploited to determine the eigenvalues of the matrix $\mathbf{A}$.

To obtain the pipe response, the gravitational load should be included in the model. Eq. (18) with gravitational load is rewritten as

$$\dot{\mathbf{Z}} = \mathbf{A}\mathbf{Z} + \mathbf{F} \tag{22}$$

with

$$\mathbf{F} = \begin{pmatrix} \mathbf{0} \\ \mathbf{M}_{\text{eq}}^{-1}\mathbf{f}_{\text{eq}} \end{pmatrix}. \tag{23}$$

The solution of Eq. (22) is given by

$$\mathbf{Z}(t) = \mathbf{e}^{\mathbf{A}t}\mathbf{Z}(0) + \int_0^t \mathbf{e}^{\mathbf{A}(t-\zeta)}\mathbf{F}\,\mathrm{d}\zeta. \tag{24}$$

The above solution Eq. (24) will be used to predict the dynamic response of the pipe.

3. Numerical results and discussions

In the collar-stiffened pipe, matrix **A** controls the nature of the system eigenvalues. Matrix **A** contains the parameters $m_f =$ fluid mass per unit length, $\rho A =$ pipe mass per unit length, $EI =$ pipe flexural rigidity, $U =$ fluid velocity relative to the pipe and $L =$ pipe length. Dimensionless quantities that contain these parameters are considered; namely, dimensionless mass ratio $\beta = m_f/(m_f + \rho A)$ and speed ratio $u = UL\sqrt{m_f/EI}$. The parameters ρA and EI are considered to be of a uniform pipe. The stability of a collar-stiffened pipe conveying fluid may be regarded as a question of how the eigenvalues λ of **A** change when the dimensionless quantities, β and u, are varied. The stable/unstable boundary is located at values of β and u which correspond to $\mathrm{Re}(\lambda) = 0$.

In this analysis, cantilever pipes of inner diameter $D_i = 14\,\text{mm}$ and outer diameter $D_o = 16\,\text{mm}$ are considered. The pipes are of length $L = 983.3\,\text{mm}$ and are fixed at the left end ($x = 0$) and free at the

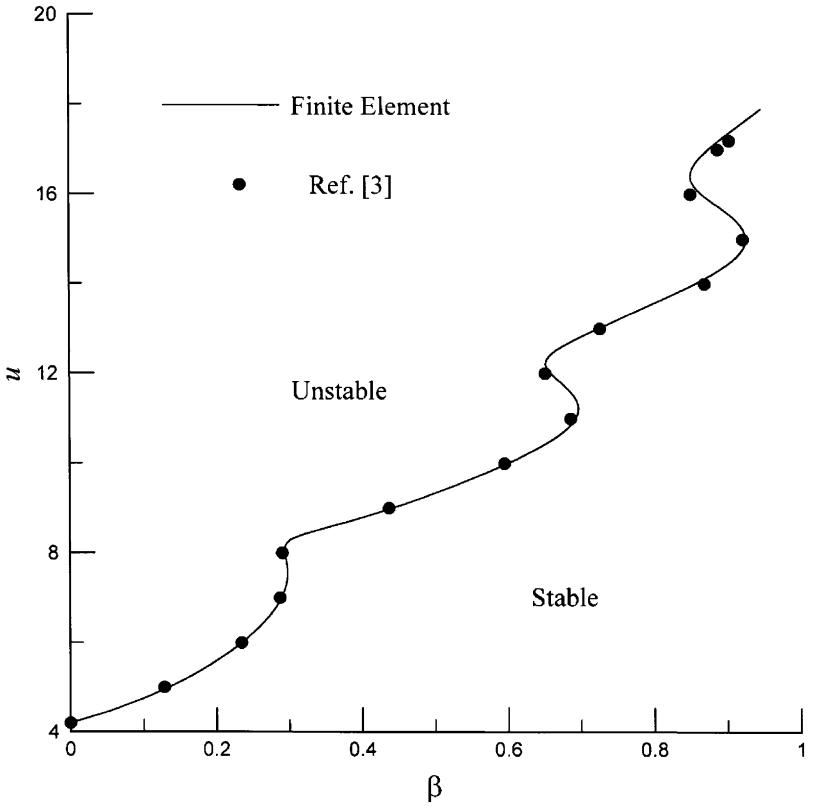

Fig. 2. Stability map of a uniform pipe: (——) finite element of the present work and (●) [3].

other end ($x = L$). The pipes are made of aluminum with Young's modulus $E = 76\,\text{GPa}$ and mass density $\rho = 2840\,\text{kg/m}^3$. The collars are also made of aluminum. Since aluminum possesses very small internal damping, the pipes internal damping is neglected $\eta \cong 0$. The pipes are exposed to flowing fluids traveling at constant speed U form the fixed end toward the free end.

The finite element model presented in the previous section is used to investigate the stability of collar-stiffened pipes with various numbers of cells, cell length ratio Ls/Lu and step factor f. The collar-stiffened pipe shown in Fig. 1(a) represents an assembly of a number of identical cells joined together in an identical fashion. Each cell is discretized into a number of finite elements. The finite elements of the collar portion have diameter larger than those in the regular portion of the cell.

To verify the validity of the finite element model, the results of the present work are compared with the previously reported results in the literature, where available. A uniform cantilever pipe is considered in the verification. This particular pipe configuration was chosen in order to make comparison with the results of Gregory and Païdoussis [3]. Fig. 2 illustrates the stability boundary (map) of a uniform pipe obtained by the present study and by Gregory and Païdoussis [3]. The results of the finite element model of the present study agree quite well with those presented in Ref. [3]. This clearly confirms the validity of the finite element model of this study.

3.1. Performance of collar-stiffened pipes

The effectiveness of the number of cells in enhancing the pipe stability is assessed for collar-stiffened pipes with two, three, four, eight and 16 cells. The considered pipes possess step factor $f = 1.25$ and cell length ratio

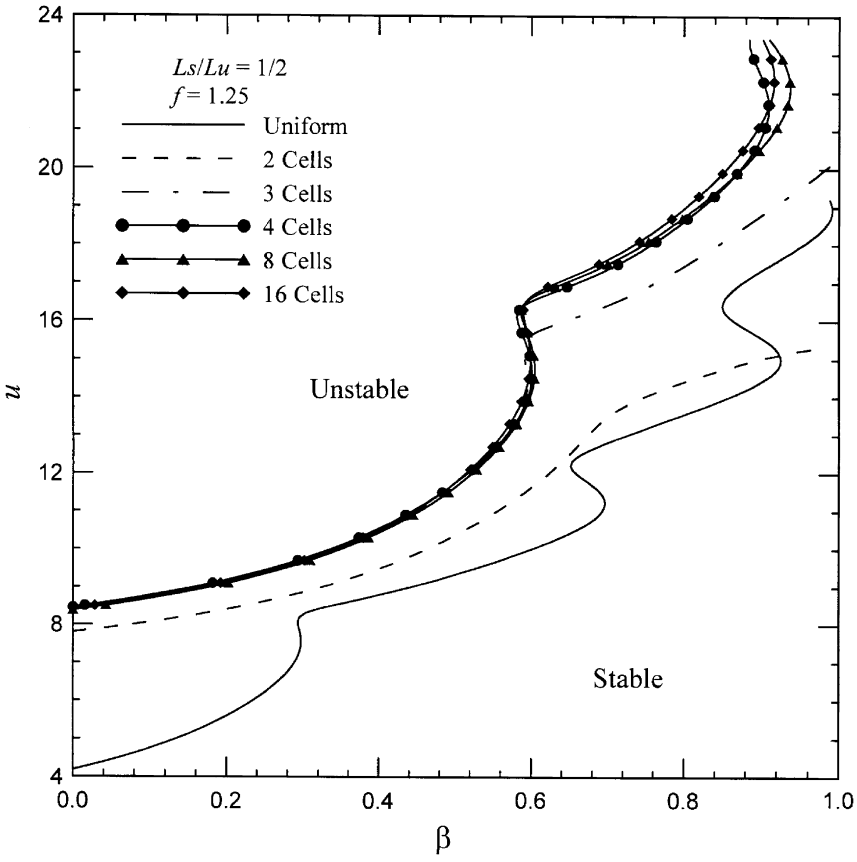

Fig. 3. Stability map of cantilever stiffened pipes for various numbers of cells. $Ls/Lu = 1/2$; ($f = 1.25$). (——) uniform pipe; (- - - -) two-cell pipe; (- · - · -) three-cell pipe; (●) four-cell pipe; (▲) eight-cell pipe; and (◆) 16-cell pipe.

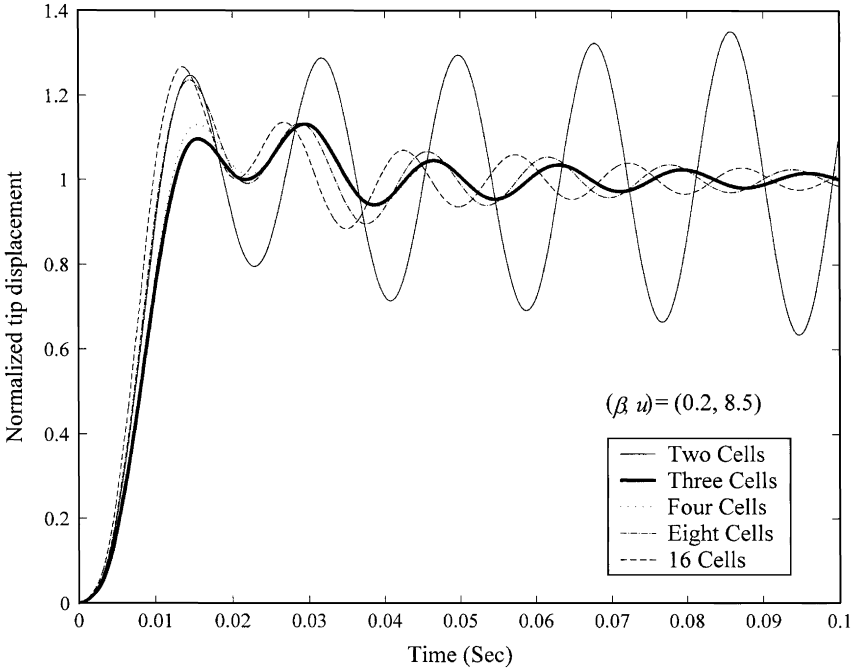

Fig. 4. Response of stiffened pipes for $\beta = 0.2$ and $u = 8.5$. (——) two-cell pipe; (▬▬) three-cell pipe; (· · · · · ·) four-cell pipe; (-.-.-), eight-cell pipe; and (- - - - -) 16-cell pipe.

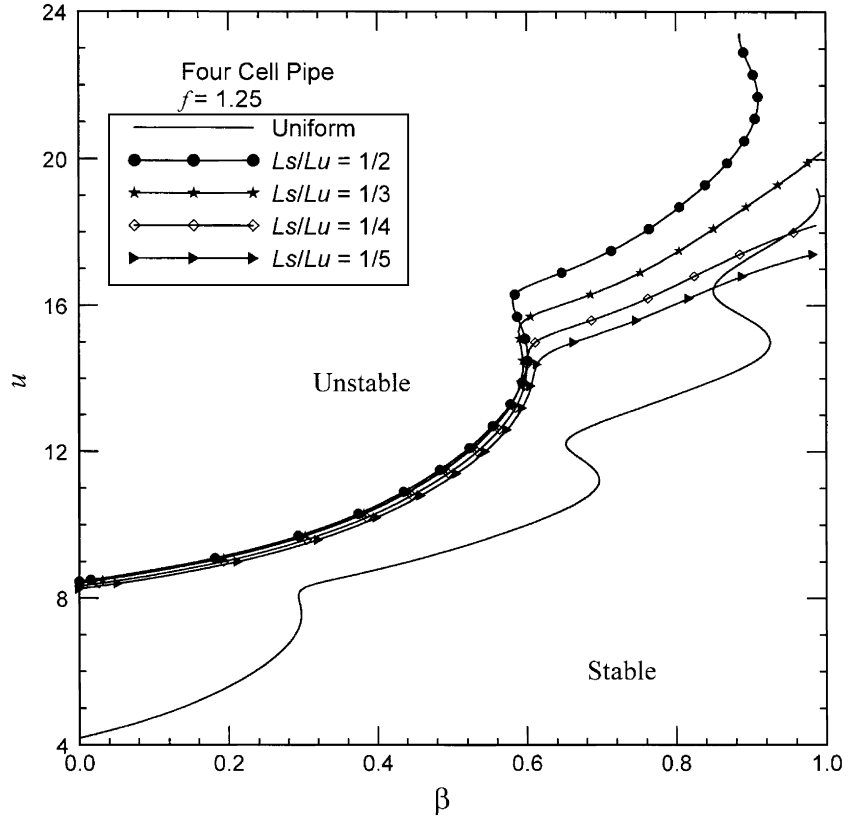

Fig. 5. Stability map of four-cell cantilever pipes for different Ls/Lu ratio. $f = 1.25$. (——) uniform pipe; (●) $Ls/Lu = 1/2$; (*) $Ls/Lu = 1/3$; (◇) $Ls/Lu = 1/4$; and (▲) $Ls/Lu = 1/5$.

$Ls/Lu = 1/2$. Fig. 3 shows the stability boundaries (map) of uniform and collar-stiffened pipes. It is clear that the presence of collars significantly improves the pipe stability characteristics when compared to a uniform pipe. It is seen that the S-shaped segments in the uniform pipe is reduced to one segment in the collar-stiffened pipes. The stability performance of four, eight and 16 cells pipes is almost identical, especially when the mass ratio β is less than 0.6. For the considered pipe parameters, this suggests that four cells are enough to provide effective enhancement in the stability characteristics of the pipe.

The time responses of the considered above collar-stiffened pipes are compared to each other. The comparison is carried out for values of dimensionless quantities of $(\beta, u) = (0.2, 8.5)$· At $t<0$, the pipe is at rest and in horizontal position. When $t \geqslant 0$, the pipe is excited by a sudden gravitational load due to the pipe and fluid weights. Fig. 4 shows the normalized tip displacements of the pipes. The normalized tip displacement represents the dynamic tip displacement divided by the static tip displacement, which is generated by only the gravitational load. For the considered values of u and β, the tip displacement of the two-cell pipe propagates with time, in accordance to the predication illustrated in Fig. 3. The vibrations of other the collar-stiffened pipes are damped out rapidly.

3.2. Effect of cell length ratio Ls/Lu on the stability

It was shown in the previous section that four cells are adequate configuration choice to assemble collar-stiffened pipe of enhanced stability characteristics. The effectiveness of the cell length ratio Ls/Lu on improving the pipe stability is evaluated in this section. The pipe consists of four cells. A value of 1.25 is taken for the step factor f. Fig. 5 shows the stability map of uniform and collar-stiffened pipes of various values of Ls/Lu ratio. It is seen that when $\beta<0.6$, the stability boundaries for considered Ls/Lu ratios are close to each other. The effect of the cell length ratio on the stability becomes significant when $\beta>0.6$. In this range, the larger the Ls/Lu ratio the better is the stability characteristics. It is interesting to note that at $\beta \geqslant 0.82$ and 0.9 the collar-stiffened pipes of $Ls/Lu = 1/5$ and $1/4$, respectively, lose stability at speed ratio u smaller than that of a uniform pipe.

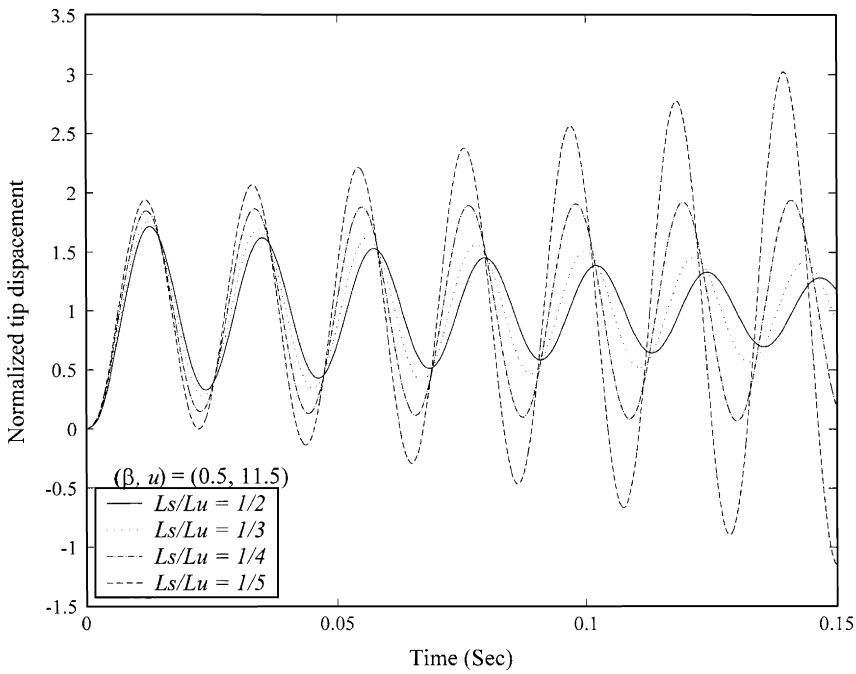

Fig. 6. Response of four-cell stiffened pipes for $\beta = 0.5$ and $u = 11.5$. (——) $Ls/Lu = 1/2$; (· · · · · ·) $Ls/Lu = 1/3$; (-.-.-) $Ls/Lu = 1/4$; and (- - - - -) $Ls/Lu = 1/5$.

The responses of the previous pipes are shown in Fig. 6 for $(\beta, u) = (0.5, 11.5)$· It is evident by inspection that the vibration amplitude of pipes of $Ls/Lu = 1/4$ and $1/5$ increase with time. On the other hand, when $Ls/Lu = 1/2$ and $1/3$ the vibration damps out. This behavior is consistent with our expectations based upon the stability map shown in Fig. 5.

3.3. Effect of step factor f on the stability

A complete assessment of the effectiveness of the stiffened pipe configuration in enhancing the pipe stability requires the consideration of the step factor f. Four cell pipes of $Ls/Lu = 1/2$ are considered. Fig. 7 shows the stability map for step factor f equals one (uniform pipe), 1.1, 1.25, 1.5 and 2. The map clearly indicates that increasing the step factor enlarges the stable region in the β–u plane. Furthermore, the map shows that the number of S-shaped segments reduces as f is increased and vanishes at a value of $f = 2$.

3.4. Eigenvalue branches

The variation paths of the eigenvalues with speed ratio u are demonstrated via the eigenvalue branches. The eigenvalue branches are used to predict the modes of vibration that are responsible for causing flutter in the pipe. When a particular eigenvalue branch crosses the imaginary axis of the root locus diagram, flutter occurs by that particular branch (mode). Figs. 8(a)–(c) shows the eigenvalue branches of the first three modes for four cells pipes with $(f, \beta) = (1.5, 0.5)$ and for various values of Ls/Lu. The numbers on the branches are the values of the speed ratio u. For a uniform pipe, the branch on which flutter occurs is that of the third mode (see Fig. 8(c)) and at $u = 9.3$. On the other hand, the collar-stiffened pipes lose stability by the second

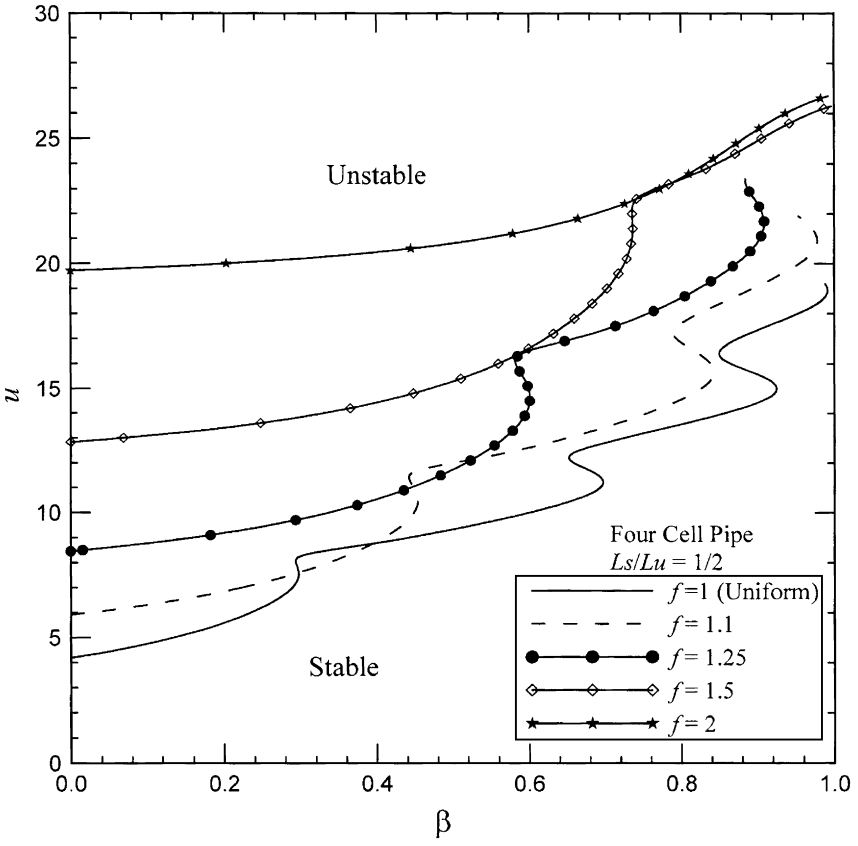

Fig. 7. Stability map of four-cell cantilever pipe for different step ratio f. (——), $f = 1$ (uniform) pipe; (----) $f = 1.1$; (●) $f = 1.25$; (◇) $f = 1.5$; and (*) $f = 2$.

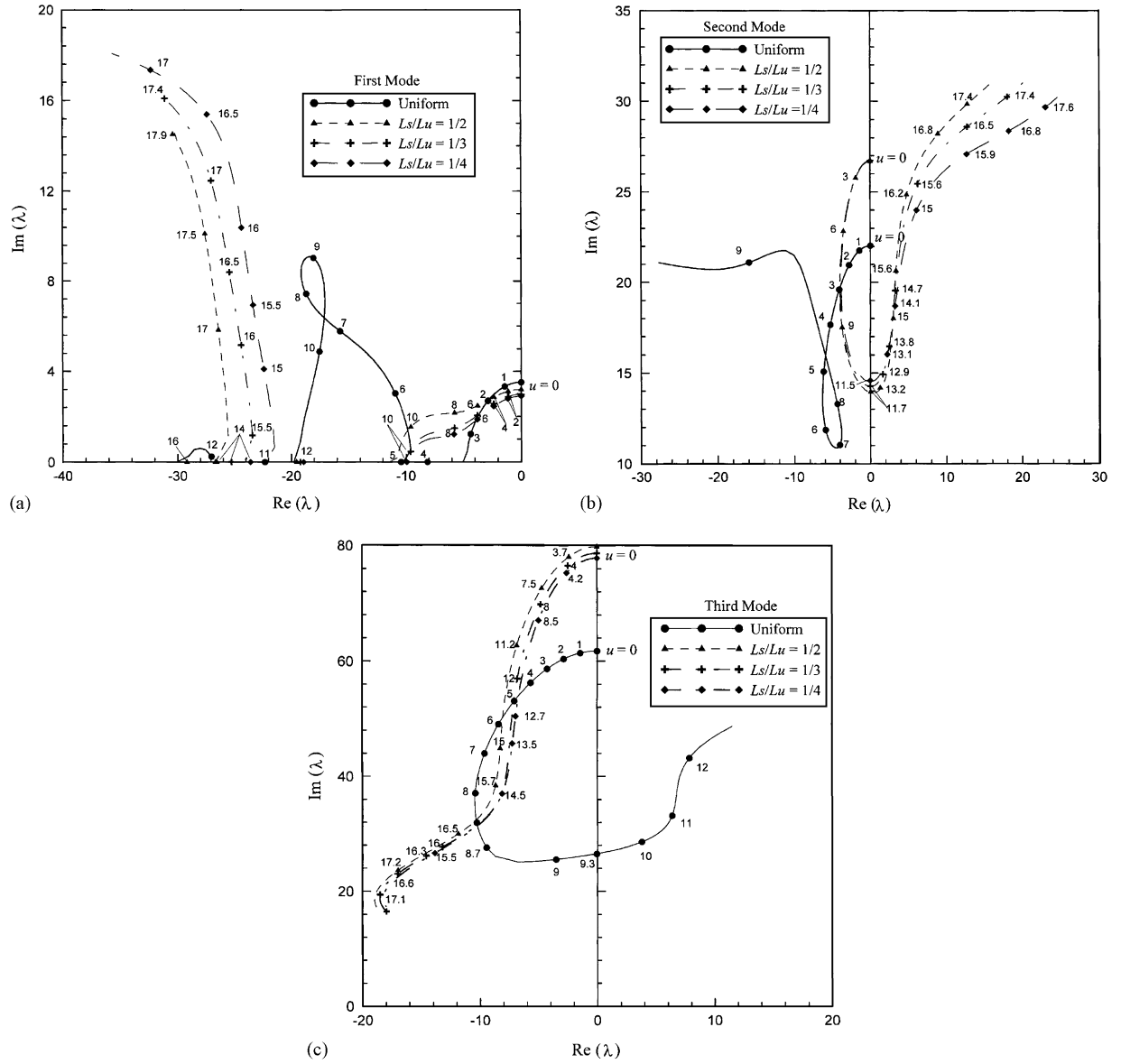

Fig. 8. Eigenvalue branches for four cells pipes with $f = 1.5$ and $\beta = 0.5$: (a) first mode; (b) second mode; and (c) third mode. (●) Uniform pipe; (▲) $Ls/Lu = 1/2$; (+) $Ls/Lu = 1/3$; and (◆) $Ls/Lu = 1/4$.

branch (see Fig. 8(b)) at $(u, Ls/Lu) = (11.5, 1/4)$, $(u, Ls/Lu) = (11.7, 1/3)$ and $(u, Ls/Lu) = (11.7, 1/2)$. These results are consistent with those shown in Figs. 3–7.

4. Conclusions

The dynamic stability of collar-stiffened pipes conveying fluid is analyzed in this work. The collar-stiffened pipes consist of cells joined together at regular intervals along the pipe length. The pipe stability is predicted by means of a finite element model, which accounts for the interaction between the flowing fluid and pipe vibration. The effects of the number of cells, cell length ratio and collar step factor on the stability characteristics are examined. Results demonstrate that collar-stiffened pipes exhibit significantly improved dynamic stability characteristics when compared to a uniform pipe. The stability characteristics of

collar-stiffened pipes with four and more cells are comparable. The effect of the cell length ratio on the stability appears to be important for large values of mass ratio. The stability results also indicate that increasing the step factor enlarges the stable region of the pipe when compared to a uniform pipe. It is also shown that the mode of vibration which is responsible for flutter in uniform and collar-stiffened pipes is not necessarily the same.

Acknowledgments

This research work was supported by the Saudi Basic Industries Corporation, SABIC (Project no. 423/26, King Saud University Annual Grant). This support is gratefully acknowledged.

References

[1] G.W. Housner, Bending vibrations of a pipe line containing flowing fluid, *ASME Journal of Applied Mechanics* 19 (1952) 205–208.
[2] T.B. Benjamin, Dynamics of a system of articulated pipes conveying fluid I: theory, *Proceedings of the Royal Society London A* 261 (1961) 457–486.
[3] R.W. Gregory, M.P. Païdoussis, Unstable oscillation of tubular cantilevers conveying fluid. I. Theory, *Proceedings of the Royal Society (London) A* 293 (1966) 512–527.
[4] R.W. Gregory, M.P. Païdoussis, Unstable oscillation of tubular cantilevers conveying fluid. II. Experiments, *Proceedings of the Royal Society (London) A* 293 (1966) 528–542.
[5] M.P. Païdoussis, *Fluid–Structure Interactions: Slender Structures and Axial Flow*, Vol. 1, Academic Press, 1998 Incorporated.
[6] M.P. Païdoussis, G.X. Li, Pipes conveying fluid: a modal dynamical problem, *Journal of Fluids and Structures* 7 (1993) 137–204.
[7] R. Pandiyan, S.C. Sinha, Analysis of time-periodic nonlinear dynamical systems undergoing bifurcations, *Nonlinear Dynamics* 8 (1995) 21–43.
[8] C. Semler, G.X. Li, M.P. Païdoussis, The non-linear equations of motion of pipes conveying fluid, *Journal of Sound and Vibration* 169 (1994) 577–599.
[9] C. Semler, M.P. Païdoussis, Parametric resonances of a cantilevered pipe conveying fluid: a nonlinear analysis, *ASME/Design Engineering Technical Conferences*. DE-Vol. 84-1 3, Part A (1995) 325–331.
[10] Z. Szabo, Bifurcation analysis of pipes conveying palsatile flow, *Periodica Polytechnica Series in Mechanical Engineering* 44 (2000) 149–160.
[11] K.Y. Maalawi, M.A. Ziada, On the static instability of flexible pipes conveying fluid, *Journal of Fluids and Structures* 16 (2002) 685–690.
[12] O.J. Aldraihem, A. Baz, Dynamic stability of stepped beams under moving loads, *Journal of Sound and Vibration* 250 (2002) 835–848.
[13] O.J. Aldraihem, A. Baz, Moving-loads-induced instability in stepped tubes, *Journal of Vibration and Control* 10 (2004) 3–23.
[14] D.B. McIver, Hamilton's principle for systems of changing mass, *Journal of Engineering Mathematics* 7 (1973) 249–261.